Unified theory for surface layers in atmospheric convective and stably stratified turbulence

I. Rogachevskii[1,2,*] N. Kleeorin[1,2], and S. Zilitinkevich[3,4]
[1]*Department of Mechanical Engineering, Ben-Gurion University of the Negev, Beer-Sheva 8410530, Israel*
[2]*Nordita, Stockholm University and KTH Royal Institute of Technology, 10691 Stockholm, Sweden*
[3]*Institute for Atmospheric and Earth System Research (INAR), University of Helsinki, 00014 Helsinki, Finland*
[4]*Finnish Meteorological Institute, 00101 Helsinki, Finland*
(Dated: December 30, 2021)

The Energy- and Flux Budget (EFB) turbulence closure theory for the atmospheric surface layers in convective and stably stratified turbulence has been developed using budget equations for turbulent energies and fluxes in the Boussinesq approximation. In the lower part of the surface layer in the atmospheric convective boundary layer (CBL), the rate of turbulence production of the turbulent kinetic energy (TKE) caused by the mean-flow surface shear and the shear of self-organised coherent structures is much larger than that caused by the buoyancy, which results in three-dimensional turbulence of very complex nature. In the upper part of the surface layer, the rate of turbulence production of TKE due to the shear is much smaller than that caused by the buoyancy, which causes unusual strongly anisotropic buoyancy-driven turbulence. Considering the applications of the obtained results to the atmospheric convective and stably stratified boundary-layer turbulence, the theoretical relationships potentially useful in modelling applications have been derived. In particular, the developed unified theory for the surface layers in turbulent convection and stably stratified turbulence allows us to determine the vertical profiles for all turbulent characteristics, including TKE, the intensity of turbulent potential temperature fluctuations, the vertical turbulent fluxes of momentum and buoyancy (proportional to potential temperature), the integral turbulence scale, the turbulent anisotropy, the turbulent Prandtl number and the flux Richardson number. This theory also yields the profiles of the mean velocity and mean potential temperature.

I. INTRODUCTION

Turbulence and the associated turbulent transport have been investigated systematically for more than hundred years in theoretical, experimental and numerical studies [1–8]. But some fundamental questions remain. This is particularly true in applications such as geophysics and astrophysics, where the governing parameter values are too large to be modelled either experimentally or numerically. The classical Kolmogorov's theory has been formulated for a neutrally stratified homogeneous and isotropic turbulence [9–12]. This turbulence is different from convective and stably stratified turbulence.

Modern understanding of atmospheric convective turbulence is based on the following [13]:

- buoyancy produces chaotic vertical plumes, which are different from small-scale turbulent eddies;
- the small-scale turbulent eddies which are produced by the mean-flow shear and the shear of self-organised coherent structures, are unstable and break down in smaller unstable eddies, thus causing the direct cascade of the turbulent kinetic energy;
- merging of small plumes into larger plumes results in an inverse energy cascade toward their conversion into the self-organized large-scale coherent structures;
- in convective turbulence, there are countergradient and nongradient turbulent transports. The gradient transport of momentum, energy, and matter implies that the turbulent flux of any quantity is determined by the product of the mean gradient of the transferred quantity and the turbulent transport coefficient. The nongradient turbulent transports means that the turbulent flux is not determined by the mean gradient of the transferred quantity.

This concept is based on various experimental, numerical and theoretical studies [14–27].

The atmospheric turbulent convective boundary layer (CBL) consists in three basic parts:

- Surface layer strongly unstably stratified and dominated by small-scale turbulence of very complex nature including usual 3-D turbulence, generated by mean-flow surface shear and structural shears (the lower part of the surface layer), and unusual strongly anisotropic buoyancy-driven turbulence (the upper part of the surface layer);
- CBL core dominated by the structural energy-, momentum- and mass-transport, with only minor contribution from usual 3-D turbulence generated by local structural shears on the background of almost zero vertical gradient of potential temperature (or buoyancy);
- turbulent entrainment layer at the CBL upper boundary, characterised by essentially stable stratification with negative (downward) turbulent flux of potential temperature (or buoyancy).

* gary@bgu.ac.il; http://www.bgu.ac.il/~gary

The goal of this paper is to develop the Energy and Flux Budget (EFB) turbulence closure for the surface layer in convective and stably stratified turbulence using budget equations for turbulent energies and fluxes. The EFB theory of turbulence closure has been previously developed for stably stratified dry atmospheric flows [28–33] and for passive scalar transport in stratified turbulence [34]. The EFB turbulence closure theory is based on the budget equations for the densities of turbulent kinetic and potential energies, and turbulent fluxes of momentum and heat. In agreement with wide experimental evidence, the EFB theory demonstrates that strong turbulence is maintained by large-scale shear in any stratification, and the "critical Richardson number", treated many years as a threshold between the turbulent and laminar regimes, actually separates two turbulent regimes: the strong turbulence typical of atmospheric boundary layers and the weak three-dimensional turbulence typical of the free atmosphere or deep ocean, and characterized by strong decrease in heat transfer in comparison to momentum transfer. The EFB theory have been verified against scarce data from the atmospheric experiments, direct numerical simulations (DNS), large-eddy simulations (LES) and laboratory experiments relevant to the steady state turbulence regime. Following the EFB closure, other turbulent closure models also do not imply a critical Richardson number [35–44].

In the present study we develop a unified theory for the surface layers in turbulent convection and stably stratified turbulence which allows us to determine the vertical profiles for all turbulent characteristics. This paper is organized as follows. In Section II we outline the EFB theory for turbulence, where we formulate governing equations for the energy and flux budget turbulence-closure theory for convective and stably stratified turbulence. In Section III we develop an unified theory for surface layers in stratified turbulence considering the steady-state and homogeneous regime of turbulence. In Section IV we consider stably stratified boundary-layer turbulence, and in Section V we study surface layers in turbulent convection. Finally, conclusions are drawn in Section VI.

II. ENERGY- AND FLUX-BUDGET EQUATIONS AND BASIC ASSUMPTIONS

We consider plain-parallel, unstably and stably stratified dry-air flow and employ the budget equations underlying turbulence-closure theory in the Boussinesq approximation. In what follows we adhere to geophysical approximation, which implies that vertical component of the mean-wind velocity is negligibly small compared to horizontal component, and horizontal gradients of all properties of the mean flow are negligibly small compared to vertical gradients.

In this section we formulate the energy and flux budget (EFB) closure theory based on the budget equations for the density of turbulent kinetic energy, the intensity of potential temperature fluctuations and turbulent fluxes of momentum and heat. In our analysis, we use budget equations for the one-point second moments to develop a mean-field theory. We do not study small-scale structure of turbulence (i.e., higher moments for turbulent quantities and intermittency). In particular, we study large-scale long-term dynamics, i.e., we consider effects in the spatial scales which are much larger than the integral scale of turbulence and in timescales which are much longer than the turbulent timescales.

The budget equations for the density of turbulent kinetic energy (TKE) $E_{\rm K} = \langle \boldsymbol{u}^2\rangle/2$ reads

$$\frac{DE_{\rm K}}{Dt} + \nabla_z \, \Phi_{\rm K} = -\tau_{iz} \, \nabla_z \overline{U}_i + \beta \, F_z - \varepsilon_{\rm K}, \qquad (1)$$

where the first term, $-\tau_{iz} \, \nabla_z \overline{U}_i$, in the right hand side of Eq. (1) is the rate of production of TKE by the vertical gradient of horizontal mean velocity $\overline{\boldsymbol{U}}(z)$, $D/Dt = \partial/\partial t + \overline{\boldsymbol{U}} \cdot \boldsymbol{\nabla}$ is the convective derivative, and $\tau_{iz} = \langle u_i \, u_z\rangle$ with $i = x, y$ are the off-diagonal components of the Reynolds stress describing the vertical turbulent flux of momentum, the angular brackets imply ensemble averaging. The second term $\beta \, F_z$ is vertical turbulent flux of buoyancy, $\beta = g/T_\ast$ is the buoyancy parameter, $\mathbf{g}$ is the gravity acceleration, $F_z = \langle u_z \, \theta\rangle$ is the vertical component of the turbulent flux of potential temperature, $\Theta = T(P_\ast/P)^{1-\gamma^{-1}}$ is the potential temperature, T is the fluid temperature with the reference value $T_\ast$, P is the fluid pressure with the reference value $P_\ast$ and $\gamma = c_{\rm p}/c_{\rm v}$ is the specific heat ratio.

The potential temperature $\Theta = \overline{\Theta} + \theta$ is characterized by the mean potential temperature $\overline{\Theta}(z)$ and fluctuations θ, the fluid velocity $\overline{\boldsymbol{U}} + \mathbf{u}$ is characterized by the mean fluid velocity [which generally includes the mean-wind velocity $\overline{\boldsymbol{U}}^{(\rm w)}(z) = (\overline{U}_x, \overline{U}_y, 0)$ and the local mean velocity $\overline{\boldsymbol{U}}^{(\rm c)}$ related to the semi-organised coherent structures in the case of CBL, i.e., large-scale convective circulations] and fluctuations $\mathbf{u} = (u_x, u_y, u_z)$. In the surface layer the effect of the semi-organised coherent structures can be very small.

The last term, $\varepsilon_{\rm K} = \nu \, \langle (\nabla_j u_i)^2\rangle$, in the right hand side of Eq. (1) is the dissipation rate of the density of the turbulent kinetic energy, where ν is the kinematic viscosity of fluid. The third-order moments $\Phi_{\rm K} = \rho_0^{-1} \langle u_z \, p\rangle + (\langle u_z \, \mathbf{u}^2\rangle - \nu \, \nabla_z \langle \mathbf{u}^2\rangle)/2$ determines the flux of $E_{\rm K}$, where the fluid pressure $P = \overline{P} + p$ is characterized by the mean pressure $\overline{P}$ and fluctuations p, and ρ_0 is the fluid density.

The budget equation for the intensity of potential temperature fluctuations $E_\theta = \langle \theta^2\rangle/2$ is

$$\frac{DE_\theta}{Dt} + \nabla_z \, \Phi_\theta = -F_z \, \nabla_z \overline{\Theta} - \varepsilon_\theta, \qquad (2)$$

where $\Phi_\theta = \left(\langle u_z \, \theta^2\rangle - \chi \, \nabla_z \langle \theta^2\rangle\right)/2$ describes the flux of E_θ and $\varepsilon_\theta = \chi \, \langle (\boldsymbol{\nabla} \theta)^2\rangle$ is the dissipation rate of the intensity of potential temperature fluctuations E_θ, and χ is the molecular temperature diffusivity.

The budget equation for the turbulent flux $F_i = \langle u_i\, \theta\rangle$ of potential temperature is given by

$$\frac{\partial F_i}{\partial t} + \nabla_z\, \mathbf{\Phi}_i^{(\mathrm{F})} = -\tau_{iz}\, \nabla_z \overline{\Theta}\, \delta_{i3} + 2\beta\, E_\theta\, \delta_{i3} - \frac{1}{\rho_0}\, \langle \theta\, \nabla_i p\rangle$$
$$-F_z\, \nabla_z \overline{U}_i - \varepsilon_i^{(\mathrm{F})}, \tag{3}$$

where δ_{ij} is the Kronecker unit tensor, $\mathbf{\Phi}_i^{(\mathrm{F})} = \langle u_i\, u_z\, \theta\rangle - \nu\, \langle\theta\, (\nabla_z u_i)\rangle - \chi\, \langle u_i\, (\nabla_z \theta)\rangle$ determines the flux of F_i, and the term $\varepsilon_i^{(\mathrm{F})} = (\nu + \chi)\, \langle (\nabla_j u_i)\, (\nabla_j \theta)\rangle$ is the dissipation rate of the turbulent heat flux. The first term, $-\tau_{iz}\, \nabla_z \overline{\Theta}\, \delta_{i3}$, in the right hand side of Eq. (3) contributes to the traditional vertical turbulent flux of potential temperature which describes the classical gradient mechanism of the turbulent heat transfer. On the other hand, the second and third terms in the right hand side of Eq. (3) describe a non-gradient contribution to the vertical turbulent flux of potential temperature. The budget equation for the vertical turbulent flux $F_z = \langle u_z\, \theta\rangle$ of potential temperature is given by

$$\frac{\partial F_z}{\partial t} + \nabla_z\, \mathbf{\Phi}_z^{(\mathrm{F})} = -2E_z\, \nabla_z \overline{\Theta} + 2\beta\, E_\theta - \frac{1}{\rho_0}\, \langle \theta\, \nabla_z p\rangle$$
$$-\varepsilon_z^{(\mathrm{F})}. \tag{4}$$

The budget equation for the off-diagonal components of the Reynolds stress $\tau_{iz} = \langle u_i\, u_z\rangle$ with $i = x, y$ reads

$$\frac{D\tau_{iz}}{Dt} + \nabla_z\, \Phi_i^{(\tau)} = -2\, E_z\, \nabla_z \overline{U}_i - \varepsilon_i^{(\tau)}, \tag{5}$$

where $E_z = \langle u_z^2\rangle/2$ is the density of the vertical turbulent kinetic energy, $\Phi_i^{(\tau)} = \langle u_i\, u_z^2\rangle + \rho_0^{-1}\, \langle p\, u_i\rangle - \nu\, \nabla_z \tau_{iz}$ describes the flux of τ_{iz}, the term $\varepsilon_i^{(\tau)} = \varepsilon_{iz}^{(\tau)} - \beta\, F_i - Q_{iz}$ in Eq. (5) is the "effective dissipation rate" of the off-diagonal components of the Reynolds stress τ_{iz}, the tensor $Q_{ij} = \rho_0^{-1}(\langle p \nabla_i u_j\rangle + \langle p \nabla_j u_i\rangle)$ and $\varepsilon_{iz}^{(\tau)} = 2\nu\, \langle (\nabla_j u_i)\, (\nabla_j u_z)\rangle$ is the molecular-viscosity dissipation rate, see below [28, 32, 34].

The budget equations for the horizontal and vertical turbulent kinetic energies $E_\alpha = \langle u_\alpha^2\rangle/2$ can be written as follows:

$$\frac{DE_\alpha}{Dt} + \nabla_z\, \Phi_\alpha = -\tau_{\alpha z}\, \nabla_z \overline{U}_\alpha + \delta_{\alpha 3}\, \beta\, F_z + \frac{1}{2} Q_{\alpha\alpha} - \varepsilon_\alpha, \tag{6}$$

where $\alpha = x, y, z$, the term $\varepsilon_\alpha = \nu\, \langle (\nabla_j u_\alpha)^2\, \rangle$ is the dissipation rate of E_α and Φ_α determines the flux of E_α. Here $\Phi_z = \rho_0^{-1} \langle u_z\, p\rangle + (\langle u_z^3\rangle - \nu\, \nabla_z \langle u_z^2\rangle)/2$ and $\Phi_{x,y} = (\langle u_z\, u_{x,y}^2\rangle - \nu\, \nabla_z \langle u_{x,y}^2\rangle)/2$. The terms $Q_{\alpha\alpha} = 2\rho_0^{-1}(\langle p \nabla_\alpha u_\alpha\rangle$ are the diagonal terms of the tensor Q_{ij}. In Eq. (6) we do not apply the summation convention for the double Greek indices. Different aspects related to budget equations (1)–(6) have been discussed in a number of publications [28–34, 37, 45–47].

The energy and flux budget turbulence closure theory assumes the following. The characteristic times of variations of the densities of the turbulent kinetic energies E_K and E_α, the intensity of potential temperature fluctuations E_θ, the turbulent flux F_i of potential temperature and the turbulent flux τ_{iz} of momentum (i.e., the off-diagonal components of the Reynolds stress) are much larger than the turbulent timescale. This allows us to obtain steady-state solutions of the budget equations (1)–(6).

Dissipation rates of the turbulent kinetic energies E_K and E_α, the intensity of potential temperature fluctuations E_θ and F_i are expressed using the Kolmogorov hypothesis, i.e., $\varepsilon_\mathrm{K} = E_\mathrm{K}/t_\mathrm{T}$, $\varepsilon_\theta = E_\theta/(C_\mathrm{p}\, t_\mathrm{T})$, $\varepsilon_{\alpha\alpha}^{(\tau)} = E_\alpha/3t_\mathrm{T}$ and $\varepsilon_i^{(\mathrm{F})} = F_i/(C_\mathrm{F}\, t_\mathrm{T})$, where $t_\mathrm{T} = \ell_z/E_z^{1/2}$ is the turbulent dissipation timescale, ℓ_z is the vertical integral scale, E_z is the vertical TKE, and C_p and C_F are dimensionless empirical constants [1, 2, 8, 9, 11].

The term $\varepsilon_i^{(\tau)} = \varepsilon_{iz}^{(\tau)} - \beta\, F_i - Q_{iz}$ in Eq. (5) is the effective dissipation rate of the off-diagonal components of the Reynolds stress τ_{iz}, where $\varepsilon_{iz}^{(\tau)} = 2\nu\, \langle (\nabla_z u_i)^2\rangle$ is the molecular-viscosity dissipation rate of τ_{iz}, that is small because the smallest eddies associated with viscous dissipation are presumably isotropic [48]. In the framework of EFB theory, the role of the dissipation of τ_{iz} is assumed to be played by the combination of terms $-\beta\, F_i - Q_{iz}$, and it is assumed that $\varepsilon_i^{(\tau)} = \tau_{iz}/(C_\tau\, t_\mathrm{T})$, where C_τ is the effective-dissipation time-scale empirical constant for stably stratified turbulence [28, 32, 34], while for a convective turbulence C_τ is a function of the flux Richardson number (see Sect. V).

We assume that the term $\rho_0^{-1}\, \langle \theta\, \nabla_z p\rangle$ in Eq. (4) for the vertical turbulent flux of potential temperature is parameterised so that $\beta\, \langle \theta^2\rangle - 2E_z\, \nabla_z \overline{\Theta} - \rho_0^{-1}\, \langle \theta\, \nabla_z p\rangle = 2C_\theta\, E_\theta$ with the positive dimensionless empirical constant C_θ which is less than 1. The justification of this assumption has been discussed in different contexts [28, 32].

III. UNIFIED THEORY FOR SURFACE LAYERS IN STRATIFIED TURBULENCE

In this section we develop the unified theory for surface layers in convective and stably stratified turbulence. The steady-state version of the budget equations for the density of turbulent kinetic energy (TKE) $E_\mathrm{K} = \langle \boldsymbol{u}^2\rangle/2$ reads

$$\nabla_z\, \Phi_\mathrm{K} = K_\mathrm{M} S^2 + \beta\, F_z - \frac{E_\mathrm{K}}{t_\mathrm{T}}, \tag{7}$$

where $t_\mathrm{T} = \ell_z/E_z^{1/2}$ is the turbulent dissipation timescale, ℓ_z is the vertical integral scale, E_z is the vertical TKE, K_M is the turbulent viscosity, S is the large-scale shear caused by the horizontal mean velocity. We assume that the flux Φ_K of TKE is $\Phi_\mathrm{K} = -C_\Phi\, \beta\, F_z\, z$, where C_Φ is the dimensionless empirical constant. The justification of this assumption is given by [13]. Equation (7) yields a nonlinear equation for the vertical profile of the normalized TKE, $\tilde{E}_\mathrm{K}(\tilde{Z}) = E_\mathrm{K}(\tilde{Z})/E_{\mathrm{K}0}$ as

$$\tilde{E}_\mathrm{K}^2 + \tilde{Z}\, \tilde{E}_\mathrm{K}^{1/2} - 1 = 0, \tag{8}$$

where the normalised height $\tilde{Z} = \ell_z/(C_* L)$, $E_{\rm K0} = u_*^2/(2C_\tau A_z)^{1/2}$, u_* is the friction velocity, $C_*^{-1} = (1 + C_\Phi)(2C_\tau)^{3/4} A_z^{1/4}$, $A_z = E_z/E_{\rm K}$ is the vertical share of TKE, and L is the local Obukhov length defined as

$$L = -\frac{\tau^{3/2}}{\beta F_z}. \tag{9}$$

For stably stratified turbulence, the vertical turbulent flux F_z of potential temperature is negative, and the local Obukhov length L is positive.

In the framework of the unified theory of surface layers, we keep the same definition (9) for L in convective turbulence as well, where the vertical turbulent flux F_z of potential temperature is positive, and L is negative. Equation (8) for the surface layer in convective turbulence ($\tilde{Z} < 0$) reads

$$\tilde{E}_{\rm K}^2 - |\tilde{Z}| \, \tilde{E}_{\rm K}^{1/2} - 1 = 0, \tag{10}$$

and it has two asymptotic solutions:

(i) for a lower part ($|\tilde{Z}| \ll 1$) of the surface convective layer, Eq. (10) yields

$$E_{\rm K} = E_{\rm K0} \left(1 + \frac{1}{2} |\tilde{Z}|\right), \tag{11}$$

(ii) for an upper part ($|\tilde{Z}| \gg 1$) of the surface convective layer, the balance of the first and the second terms in Eq. (8) yields $\tilde{E}_{\rm K} = \tilde{Z}^{2/3}$, i.e.,

$$E_{\rm K} = E_{\rm K0} \, \tilde{Z}^{2/3}. \tag{12}$$

Note that as follows from the definition of $\tilde{Z} = \ell_z/(C_* L)$, the ratio z/L for convective turbulence is

$$\frac{z}{L} = \frac{\tilde{Z}}{\kappa_0 \, (1 + C_\Phi)}, \tag{13}$$

where $\ell_z = C_\ell \, z$, $\kappa_0 = 0.4$ is the von Karman constant and $C_\ell = \kappa_0 \, (2C_\tau)^{-3/4} A_z^{-1/4}$. Note that generally, Eq. (13) can be valid also for arbitrary z, but in this case C_ℓ should be a function of height (see Section V).

For stably stratified turbulence ($\tilde{Z} > 0$), Eq. (8) has two asymptotic solutions:

(i) for a lower part ($\tilde{Z} \ll 1$) of the surface layer, Eq. (8) yields

$$\tilde{E}_{\rm K} = 1 - \frac{\tilde{Z}}{2} + \frac{\tilde{Z}^2}{8}, \tag{14}$$

(ii) for an upper part ($\tilde{Z} \gg 1$) of the surface layer, it is

$$\tilde{E}_{\rm K} = \tilde{Z}^{-2} \left(1 - 2\tilde{Z}^{-4}\right). \tag{15}$$

In Fig. 1 we show a numerical solution of Eq. (8). In particular, in Fig. 1 we plot the normalized turbulent kinetic energy $\tilde{E}_{\rm K} = E_{\rm K}/E_{\rm K0}$ versus $\tilde{Z}$ for convective ($\tilde{Z} < 0$) and stably stratified ($\tilde{Z} > 0$) turbulence. This numerical solution is in a good agreement with the above asymptotic solutions for convective and stably stratified turbulence.

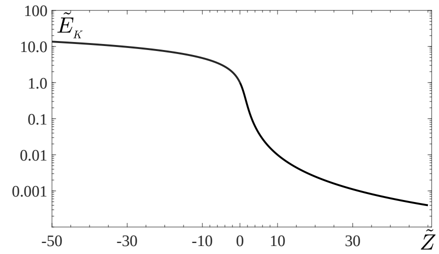

FIG. 1. The normalized turbulent kinetic energy $\tilde{E}_{\rm K} = E_{\rm K}/E_{\rm K0}$ versus $\tilde{Z}$ for convective and stably stratified turbulence.

Next, we use the familiar down-gradient formulation of the vertical turbulent flux of momentum which follows from Eq. (5), i.e., the turbulent fluxes of the momentum are

$$\tau_{iz} = -K_{\rm M} \, \nabla_z \overline{U}_i, \quad i = x, y, \tag{16}$$

$$K_{\rm M} = 2C_\tau \, t_{\rm T} \, E_z = 2C_\tau \, \ell_z \, E_z^{1/2}, \tag{17}$$

where $K_{\rm M}$ is the turbulent viscosity.

Now we define the flux Richardson number as

$${\rm Ri_f} = -\frac{\beta \, F_z}{K_{\rm M} S^2}, \tag{18}$$

so that for stably stratified turbulence, ${\rm Ri_f}$ is positive and varies from 0 to the limiting value $R_\infty = 0.2$ at very large gradient Richardson number ${\rm Ri} \gg 1$, where the gradient Richardson number, Ri, is defined as

$${\rm Ri} = \frac{N^2}{S^2}, \tag{19}$$

$S^2 = (\nabla_z \overline{U}_x)^2 + (\nabla_z \overline{U}_y)^2$ is the squared mean velocity shear, $N^2 = \beta \, \nabla_z \overline{\Theta}$ and N is the Brunt-Väisälä frequency. In the framework of the unified theory of surface layers, we keep the same definition (18) for the flux Richardson number in turbulent convection, so that ${\rm Ri_f}$ is negative in turbulent convection, and its absolute value is not limited and can be large.

Equations (9) and (18) allow us to relate the turbulent viscosity $K_{\rm M}$ with the flux Richardson number ${\rm Ri_f}$ as

$$K_{\rm M} = {\rm Ri_f} \, \tau^{1/2} \, L, \tag{20}$$

where

$$\tau = \left(\tau_{xz}^2 + \tau_{yz}^2\right)^{1/2} = K_{\rm M} \, S, \tag{21}$$

and in the surface layers $\tau = u_*^2$. Using Eqs. (17) and (20), we rewrite the flux Richardson number as

$${\rm Ri_f} = (1 + C_\Phi)^{-1} \, \tilde{Z} \, \tilde{E}_{\rm K}^{1/2}. \tag{22}$$

Equations (20) and (21) allow us to relate the large-scale shear S with the flux Richardson number as

$$S = \frac{\tau^{1/2}}{L \, {\rm Ri_f}}. \tag{23}$$

Using Eqs. (17), we rewrite Eq. (7) as the dimensionless ratio

$$\left(\frac{E_{\rm K}}{\tau}\right)^2 = \frac{1-{\rm Ri_f}\,(1+C_\Phi)}{2C_\tau\, A_z}. \tag{24}$$

By means of Eqs. (17), (20) and (24), we obtain the normalized vertical integral scale ℓ_z as the function of the flux Richardson number:

$$\frac{\ell_z}{L} = \frac{(2C_\tau)^{-3/4}\, A_z^{-1/4}\, {\rm Ri_f}}{[1-{\rm Ri_f}\,(1+C_\Phi)]^{1/4}}, \tag{25}$$

where $1-{\rm Ri_f}\,(1+C_\Phi)>0$. This condition implies that $C_\Phi < R_\infty^{-1}-1$. For stably stratified turbulence $R_\infty = 0.2$, so that $C_\Phi < 4$. Thus, the normalised height $\tilde Z = \ell_z/(C_*\, L)$ as the function of the flux Richardson number reads

$$\tilde Z = \frac{{\rm Ri_f}\,(1+C_\Phi)}{[1-{\rm Ri_f}\,(1+C_\Phi)]^{1/4}}. \tag{26}$$

Note also that using Eq. (26) we can rewrite Eq. (25) as

$$\frac{\ell_z}{L} = \frac{C_\ell\, \tilde Z}{\kappa_0\,(1+C_\Phi)}. \tag{27}$$

Since convective turbulence is strongly different from stably stratified turbulence, the behaviour of the flux Richardson number ${\rm Ri_f} \propto \tilde Z\, \tilde E_{\rm K}^{1/2}$ is different. In convection, both, the buoyancy and large-scale shear produce convective turbulence, so that the flux Richardson number can be large. Contrary, in stably stratified turbulence the large-scale shear produces turbulence, and the buoyancy decreases TKE, so that the flux Richardson number is limited by some value, ${\rm R}_\infty = 0.2$. In the presence of internal gravity waves this value can increase in several times [30, 33].

Equations (8) and (22) yield the normalized turbulent kinetic energy $\tilde E_{\rm K} = E_{\rm K}/E_{\rm K0}$ as a function of the flux Richardson number as

$$\tilde E_{\rm K} = [1-(1+C_\Phi)\,{\rm Ri_f}]^{1/2}\,. \tag{28}$$

This implies that the normalized turbulent kinetic energy $\tilde E_{\rm K}$ in stably stratified turbulence decreases up to the minimum value

$$\tilde E_{\rm K}^{\rm min} = [1-(1+C_\Phi)\,{\rm R}_\infty]^{1/2}. \tag{29}$$

As follows from Eq. (22), the function $\tilde Z\, \tilde E_{\rm K}^{1/2} \le (1+C_\Phi)\,{\rm R}_\infty$, so that the maximum value of the height $\tilde Z^{\rm max}$ in stably stratified turbulence is

$$\tilde Z^{\rm max} = \frac{{\rm R}_\infty\,(1+C_\Phi)}{[1-{\rm R}_\infty\,(1+C_\Phi)]^{1/4}}. \tag{30}$$

Since in convective turbulence, the flux Richardson number is negative, the normalized turbulent kinetic energy, $\tilde E_{\rm K} = [1+(1+C_\Phi)\,|{\rm Ri_f}|]^{1/2}$, increases with the flux Richardson number.

Now we derive expression for the turbulent Prandtl number, ${\rm Pr}_{_{\rm T}} = K_{\rm M}/K_{\rm H}$. To this end, we use the steady-state versions of Eqs. (2) and (4):

$$F_z\, \nabla_z \overline{\Theta} + \frac{E_\theta}{C_{\rm p}\, t_{\rm T}} = 0, \tag{31}$$

$$2E_z\, \nabla_z \overline{\Theta} - 2C_\theta\, \beta\, E_\theta + \frac{F_z}{C_{\rm F}\, t_{\rm T}} = 0. \tag{32}$$

Equations (31)–(32) and the expression for the turbulent heat flux, $F_z = -K_{\rm H}\, \nabla_z \overline{\Theta}$, yield the turbulent heat conductivity $K_{\rm H}$ as

$$K_{\rm H} = 2C_{\rm F}\, t_{\rm T}\, E_z \left[1 + \frac{C_\theta\, C_{\rm p}\, t_{\rm T}\, \beta F_z}{E_z}\right]. \tag{33}$$

By means of Eq. (7) for TKE,

$$E_{\rm K} = K_{\rm M}\, S^2\, t_{\rm T}\, [1-{\rm Ri_f}\,(1+C_\Phi)], \tag{34}$$

and Eq. (18) for ${\rm Ri_f}$, we derive the identity for the dimensionless ratio as

$$\frac{\beta\, F_z\, t_{\rm T}}{E_z} = -\frac{{\rm Ri_f}}{A_z\,[1-{\rm Ri_f}\,(1+C_\Phi)]}. \tag{35}$$

Thus, Eqs. (17), (33) and (35) yield the turbulent Prandtl number, ${\rm Pr}_{_{\rm T}} = K_{\rm M}/K_{\rm H}$ as

$${\rm Pr}_{_{\rm T}} = {\rm Pr}_{_{\rm T}}^{(0)} \, \left[1 - \frac{C_\theta\, C_{\rm p}\, {\rm Ri_f}}{A_z\,[1-{\rm Ri_f}\,(1+C_\Phi)]}\right]^{-1}, \tag{36}$$

where ${\rm Pr}_{_{\rm T}}^{(0)} = C_\tau/C_{\rm F}$ is the turbulent Prandtl number for a non-stratified turbulence when the mean potential temperature gradient vanishes. The gradient Richardson number Ri and the flux Richardson number ${\rm Ri_f}$ are related as ${\rm Ri} = {\rm Ri_f}\, {\rm Pr}_{_{\rm T}}$.

Using Eqs. (31)–(32), we determine the level of temperature fluctuations characterised by the dimensional ratio E_θ/θ_*^2 as

$$\frac{E_\theta}{\theta_*^2} = C_{\rm p}\,(2C_\tau\, A_z)^{-1/2}\; {\rm Pr}_T\, \tilde E_{\rm K}^{-1}, \tag{37}$$

where $\theta_* = |F_z|/u_* = u_*^2/\beta\,|L|$. Equation (23), and expressions for the friction velocity, $u_*^2 = K_{\rm M}\, S$, and the turbulent heat flux, $F_z = -K_{\rm H}\, \nabla_z \overline{\Theta}$, yield the vertical gradient of the mean potential temperature as

$$\nabla_z \overline{\Theta} = \frac{\theta_*\, {\rm Pr}_{_{\rm T}}}{|L|\, {\rm Ri_f}}. \tag{38}$$

The steady-state version of Eq. (3) for homogeneous turbulence yields the horizontal turbulent flux F_i of potential temperature:

$$F_i = -C_{\rm F}\, t_{\rm T}\, F_z\, \nabla_z \overline{U}_i, \quad i = x, y. \tag{39}$$

Since in convective turbulence the vertical turbulent flux F_z is positive, the horizontal turbulent flux F_i of potential temperature is directed opposite to the wind velocity $\overline{U}_i$, i.e., Eq. (39) describes the counter-wind horizontal turbulent flux in convective turbulence. Contrary, in a stably stratified turbulence the vertical turbulent flux F_z is negative, so that Eq. (39) determines the co-wind horizontal turbulent flux.

The physics of the counter-wind turbulent flux is the following. Let us consider horizontally homogeneous, sheared convective turbulence. With increasing height in convection, the mean shear velocity $\overline{U}_x$ increases and mean potential temperature $\overline{\Theta}$ decreases, where we consider the case when the mean velocity $\overline{U}_i$ is directed along the x-axis. Thus, uprising fluid particles produce positive fluctuations of potential temperature, $\theta > 0$ [since $\partial\theta/\partial t \propto -(\boldsymbol{u}\cdot\boldsymbol{\nabla})\overline{\Theta}$], and negative fluctuations of horizontal velocity, $u_x < 0$ [since $\partial u_x/\partial t \propto -(\boldsymbol{u}\cdot\boldsymbol{\nabla})\overline{U}_x$]. This causes negative horizontal temperature flux: $u_x\,\theta < 0$. Likewise, sinking fluid particles produce negative fluctuations of potential temperature, $\theta < 0$, and positive fluctuations of horizontal velocity, $u_x > 0$, also causing negative horizontal temperature flux $u_x\,\theta < 0$. This implies that the net horizontal turbulent flux is negative, $\langle u_x\,\theta\rangle < 0$, in spite of a zero horizontal mean temperature gradient. Thus, the counter-wind turbulent flux of potential temperature describes modification of the potential-temperature flux by the non-uniform velocity field. The counter-wind or co-wind turbulent fluxes are associated with non-gradient turbulent transport of heat.

Let us find dependence of the horizontal turbulent flux F_i of potential temperature on the flux Richardson number. To this end we use the identity,

$$\left(S\,t_{\rm T}\right)^2 = \frac{1}{2\,C_\tau\,A_z\,[1-{\rm Ri_f}\,(1+C_\Phi)]}, \tag{40}$$

that is derived by means of Eqs. (17), (21) and (24). Therefore, the ratio of the horizontal and vertical turbulent fluxes of potential temperature, F_x/F_z, is given by

$$\frac{F_x}{F_z} = -C_{\rm F}\,\left(2\,C_\tau\,A_z\right)^{-1/2}\,\Big[1-{\rm Ri_f}\,(1+C_\Phi)\Big]^{-1/2}. \tag{41}$$

Most of the results obtained in this section depend on the vertical share of TKE, $A_z \equiv E_z/E_{\rm K}$. Let us determine the vertical share of TKE, A_z. In a sheared turbulence, the mean velocity shear generates the energy of longitudinal velocity fluctuations E_x, which in turns feeds the transverse E_y and the vertical E_z components of turbulent kinetic energy. The inter-component energy exchange term $Q_{\alpha\alpha}$ in Eq. (6) is traditionally parameterized through the "return-to-isotropy" hypothesis by [49]. However, the temperature stratified turbulence is usually anisotropic, and the inter-component energy exchange term $Q_{\alpha\alpha}$ should depend on the flux Richardson number ${\rm Ri_f}$.

Here we adopt a different model for the inter-component energy exchange term $Q_{\alpha\alpha}$ which generalizes the "return-to-isotropy" hypothesis to the case of the convective and stably stratified turbulence. Here we use the normalised flux Richardson number ${\rm Ri_f}/R_\infty$ that is varying from 0 for a non-stratified turbulence to 1 for a strongly stratified turbulence, where the limiting value of the flux Richardson number, ${\rm R}_\infty \equiv {\rm Ri_f}|_{\rm Ri\to\infty}$, is defined for very strong stratifications when the gradient Richardson number ${\rm Ri}\to\infty$. The model for the inter-component energy exchange term $Q_{\alpha\alpha}$ is described by

$$Q_{xx} = -\frac{2(1+C_{\rm r})}{3t_{\rm T}}\,\left(3E_x - E_{\rm int}\right), \tag{42}$$

$$Q_{yy} = -\frac{2(1+C_{\rm r})}{3t_{\rm T}}\,\left(3E_y - E_{\rm int}\right), \tag{43}$$

$$Q_{zz} = -\frac{2(1+C_{\rm r})}{3t_{\rm T}}\,\left(3E_z - 3E_{\rm K} + 2E_{\rm int}\right), \tag{44}$$

where

$$E_{\rm int} = E_{\rm K} + \frac{\rm Ri_f}{R_\infty}\,\left(\frac{C_{\rm r}}{1+C_{\rm r}}\right)\,E_z, \tag{45}$$

and $C_{\rm r}$ is the dimensionless empirical constant. When ${\rm Ri_f}=0$, Eqs. (42)–(45) describe the "return-to-isotropy" hypothesis [49]. To derive equation for the vertical share of TKE, we use the steady-state version of Eq. (6) for E_z,

$$\nabla_z\,\Phi_z = \beta\,F_z + \frac{1}{2}Q_{zz} - \frac{E_{\rm K}}{3t_{\rm T}}, \tag{46}$$

where we assume that the flux Φ_z of the vertical TKE is given by $\Phi_z = -C_z\,\beta\,F_z\,z$, and C_z is the dimensionless empirical constant. Thus, by means of Eqs. (35) and (44)–(46), we determine the vertical share of TKE $A_z \equiv E_z/E_{\rm K}$ as a function of the flux Richardson number:

$$A_z({\rm Ri_f}) = A_z^{(0)} - {\rm Ri_f}\left[\frac{(1-3A_z^{(0)})\,(1+C_z)}{1-{\rm Ri_f}\,(1+C_\Phi)} - \frac{2A_z^{(0)}}{{\rm R}_\infty}\right] \times\left[1-2A_z^{(0)}\,\frac{\rm Ri_f}{{\rm R}_\infty}\right]^{-1}. \tag{47}$$

According to Eq. (47), the vertical share A_z of TKE for a non-stratified turbulence is $(A_z)_{\rm Ri\to 0} \equiv A_z^{(0)} = C_{\rm r}/3(1+C_{\rm r})$. Usually in surface layers in convective turbulence, $|{\rm Ri_f}| \ll |{\rm R}_\infty|$. This implies that the vertical share of TKE A_z in a convective turbulence is given by

$$A_z({\rm Ri_f}) = A_z^{(0)} + (1-3A_z^{(0)})\,\frac{|{\rm Ri_f}|\,(1+C_z)}{1+|{\rm Ri_f}|\,(1+C_\Phi)}. \tag{48}$$

In convective turbulence for large $|{\rm Ri_f}| \gg 1$, the vertical share of TKE $A_z \to 1$ [13]. This condition yields

$$\frac{1+C_z}{1+C_\Phi} = \frac{1-A_z^{(0)}}{1-3A_z^{(0)}}. \tag{49}$$

Therefore, the vertical share of TKE A_z in stably stratified turbulence is

$$A_z({\rm Ri_f}) = A_z^{(0)} - {\rm Ri_f}\left[\frac{1-A_z^{(0)}}{(1+C_\Phi)^{-1}-{\rm Ri_f}} - \frac{2A_z^{(0)}}{{\rm R}_\infty}\right] \times\left[1-2A_z^{(0)}\,\frac{\rm Ri_f}{{\rm R}_\infty}\right]^{-1}, \tag{50}$$

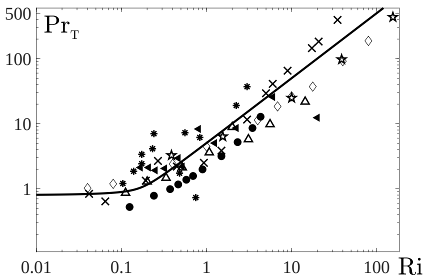

FIG. 2. The turbulent Prandtl number $\mathrm{Pr_T}$ versus the gradient Richardson number Ri for stably stratified turbulence. Comparison with data of meteorological observations: slanting black triangles [50], snowflakes [51]; laboratory experiments: slanting crosses [52], six-pointed stars [53], black circles [54]; DNS: five-pointed stars [55]; LES: triangles [32].

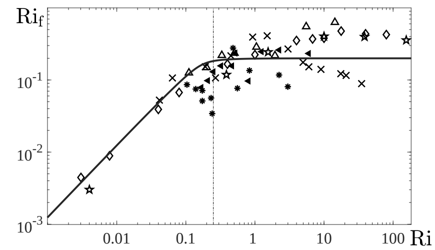

FIG. 3. The flux Richardson number $\mathrm{Ri_f}$ versus the gradient Richardson number Ri for stably stratified turbulence. Comparison with data of meteorological observations: slanting black triangles [50], snowflakes [51]; laboratory experiments: slanting crosses [52], six-pointed stars [53], black circles [54]; DNS: five-pointed stars [55]; LES: triangles [32].

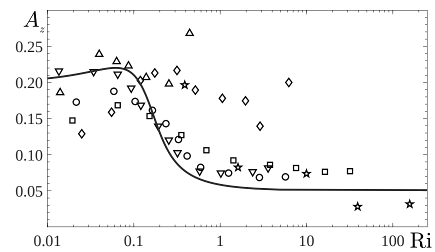

FIG. 4. The vertical share of TKE $A_z \equiv E_z/E_{\rm K}$ versus the gradient Richardson number Ri for stably stratified turbulence. Comparison with data of meteorological observations: squares [56], circles [57], overturned triangles [58, 59], six-pointed stars [58, 59]; laboratory experiments: six-pointed stars [53]; DNS: five-pointed stars [55].

while in convective turbulence (where $|\mathrm{Ri_f}| \ll |\mathrm{R}_\infty|$ and $\mathrm{Ri_f} < 0$), the vertical share of TKE A_z is given by

$$A_z(\mathrm{Ri_f}) = A_z^{(0)} + \frac{\left(1 - A_z^{(0)}\right)|\mathrm{Ri_f}|}{(1 + C_\Phi)^{-1} + |\mathrm{Ri_f}|}. \tag{51}$$

Assuming that the horizontal shares of TKE $A_x = A_y = 1 - A_z$, we determine the horizontal components of TKE as

$$E_x = E_y = E_{\rm K}\,(1 - A_z), \tag{52}$$

where $A_x = E_x/E_{\rm K}$ and $A_y = E_y/E_{\rm K}$.

IV. STABLY STRATIFIED BOUNDARY-LAYER TURBULENCE

In this section we apply results obtained in Section III to a stably stratified turbulence. For illustration, in Figs. 2–4 we show the dependencies of the following parameters on the gradient Richardson number Ri for stably stratified turbulence: (i) the turbulent Prandtl number $\mathrm{Pr_T}(\mathrm{Ri})$, given by Eq. (36), and shown in Fig. 2; (ii) the flux Richardson number $\mathrm{Ri_f}(\mathrm{Ri})$, given by Eq. (22), and shown in Fig. 3; and (iii) the vertical share of TKE $A_z(\mathrm{Ri}) \equiv E_z/E_{\rm K}$, given by Eq. (50), and shown in Fig. 4.

The theoretical Ri-dependencies are compared with data of meteorological observations, laboratory experiments, DNS and LES. Data for $\mathrm{Pr_T}(\mathrm{Ri})$ at small gradient Richardson number Ri in Fig. 2 are consistent with the commonly accepted estimate of $\mathrm{Pr_T^{(0)}} = 0.8$ [60–62]. The flux Richardson number $\mathrm{Ri_f}$ in the steady-state regime can only increase with the increasing Ri, but obviously cannot exceed unity. Hence it should tend to a finite asymptotic limit (estimated as $\mathrm{R}_\infty = 0.2$), which corresponds to the asymptotically linear Ri-dependence of $\mathrm{Pr_T}$. Since the turbulent Prandtl number, the gradient Richardson number Ri and the flux Richardson number are related as $\mathrm{Pr_T} = \mathrm{Ri}/\mathrm{Ri_f}$, the turbulent Prandtl number for strong stratifications is given by $\mathrm{Pr_T} = \mathrm{Pr_T^{(0)}} + \mathrm{Ri}/\mathrm{R}_\infty$. Figure 3 shows that the flux Richardson number $\mathrm{Ri_f}$ at the gradient Richardson number $\mathrm{Ri} > 1$ levels off at the limiting value, $\mathrm{Ri_f} = \mathrm{R}_\infty = 0.2$. Figure 4 demonstrates that the vertical share of TKE A_z levels off at $\mathrm{Ri} > 1$ as well. Figures 2–4 demonstrate reasonable agreement between theoretical predictions based on the EFB turbulence theory and data obtained from atmospheric and laboratory experiments, LES and DNS.

Let us discuss the choice of the dimensionless empirical constants [32, 34]. There are two well-known universal constants: the limiting value of the flux Richardson number $R_\infty = 0.2$ for an extremely strongly stratified turbulence (i.e., for $\mathrm{Ri} \to \infty$) and the turbulent Prandtl number $\mathrm{Pr}_T^{(0)} = 0.8$ for a nonstratified turbulence (i.e., for $\mathrm{Ri} \to 0$). The constant $C_{\rm p}$ describes the deviation of the dissipation timescale of $E_\theta = \langle\theta^2\rangle/2$ from the dissipation timescale of TKE. The constant C_θ is given by $C_\theta = A_z^{(\infty)}[(1 - \mathrm{R}_\infty(1 + C_\phi)]/(C_{\rm p}\mathrm{R}_\infty)$ [see Eq. (36)]. We use here the following values of the non-dimensional empirical constants: $C_{\rm p} = 0.417$, $C_\theta = 0.372$, $C_\phi = 0.899$, $\kappa_0 = 0.4$, $\mathrm{Pr_T^{(0)}} = 0.8$, $A_z^{(0)} = 0.2$, $A_z^{(\infty)} = 0.05$. These constants are determined from the data of numerous meteorological observations, laboratory experiments, direct numerical simulations (DNS) and large eddy simulations (LES) [28, 32, 43, 50–56, 58, 63, 64]. The parameter $C_\tau = 0.1$ for stably stratified turbulence and $C_{\rm F} = C_\tau/{\rm Pr}_{T}^{(0)} = 0.125$. For convective turbulence, C_τ is the function of the flux Richardson number ${\rm Ri_f}$ (see Section V).

Considering the applications of the obtained results to the atmospheric stably stratified boundary-layer turbulence, we derive below the theoretical relationships potentially useful in modelling applications. There are two well-known results for the wind shear in stably stratified turbulence: $S = \tau^{1/2}/(\kappa_0\, z)$ at $\varsigma \ll 1$, that yields the log-profile for the mean velocity, and $S = \tau^{1/2}/({\rm R}_\infty\, L)$ when $\varsigma \gg 1$, that follows from Eq. (23). Here $\varsigma = \int_0^z dz'/L(z')$ is the dimensionless height based on the local Obukhov length scale $L(z) = \tau^{3/2}(z)/[-\beta\, F_z(z)]$, and $\kappa_0 = 0.4$ is the von Karman constant. For surface layer in stably stratified turbulence (defined as the lower layer which is 10 % of the turbulent boundary layer), the Obukhov length scale L is independent of z and the dimensionless height $\varsigma = z/L$.

The straightforward interpolation between these two asymptotic results for the wind shear, $S(\varsigma)$,

$$S = \frac{\tau^{1/2}}{L} \left(R_\infty^{-1} + \frac{1}{\kappa_0\, \varsigma}\right), \tag{53}$$

yields the vertical profile of the turbulent viscosity $K_{\rm M}(\varsigma) = \tau/S$ as

$$K_{\rm M} = \tau^{1/2}\, L\, \frac{\kappa_0\, \varsigma}{1 + R_\infty^{-1}\, \kappa_0\, \varsigma}. \tag{54}$$

The vertical profile of the flux Richardson number ${\rm Ri_f}(\varsigma)$ is obtained using Eqs. (20) and (54):

$${\rm Ri_f} = \frac{\kappa_0\, \varsigma}{1 + R_\infty^{-1}\, \kappa_0\, \varsigma}. \tag{55}$$

Equation (55) yields the expression for ς as

$$\varsigma = \frac{{\rm Ri_f}}{\kappa_0\, (1 - {\rm Ri_f}/R_\infty)}. \tag{56}$$

The vertical share of TKE $A_z(\varsigma) \equiv E_z/E_{\rm K}$ is

$$A_z = A_z^{(0)} + \left[1 + {\rm R}_\infty\, (\kappa_0\, \varsigma)^{-1} - 2A_z^{(0)}\right]^{-1} \biggl[2A_z^{(0)} + \frac{1 - A_z^{(0)}}{[1 + {\rm R}_\infty\, (\kappa_0\, \varsigma)^{-1}]^{-1} - [{\rm R}_\infty\, (1 + C_\Phi)]^{-1}}\biggr], \tag{57}$$

and the vertical profiles of the turbulent Prandtl number ${\rm Pr}_{T}(\varsigma)$ is given by:

$${\rm Pr_{\scriptscriptstyle T}} = {\rm Pr_{\scriptscriptstyle T}^{(0)}} \left[1 - \frac{C_\theta\, C_{\rm p}}{A_z\, \left[{\rm R}_\infty^{-1} + (\kappa_0\, \varsigma)^{-1} - (1 + C_\Phi)\right]}\right]^{-1}. \tag{58}$$

The gradient Richardson number Ri and the flux Richardson number ${\rm Ri_f}$ are related as ${\rm Ri}(\varsigma) = {\rm Ri_f}(\varsigma)\, {\rm Pr_{\scriptscriptstyle T}}(\varsigma)$.

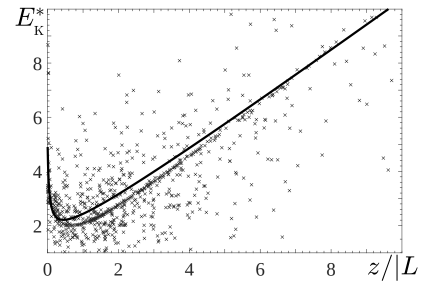

FIG. 5. The normalized turbulent kinetic energy $E_{\rm K}^* = E_{\rm K}/u_*^2$ versus z/L obtained in the EFB theory (solid line) which is compared with the data obtained from meteorological observations at the Eureka station located in the Canadian territory of Nunavut [68] in the conditions of long-lived convective boundary layer typical of the arctic summer.

Equations (54)–(58) are in agreement with [65] and [66] similarity theories, i.e., the concept of similarity of turbulence in terms of the dimensionless height $\varsigma = \int_0^z dz'/L(z')$. The Monin-Obukhov similarity theory was designed for the surface layer, where the turbulent fluxes of momentum τ, heat F_z and other scalars, as well as the length scale L, are approximated by their surface values. [66] extended the similarity theory to the entire stably stratified boundary layer employing local z-dependent values of the turbulent fluxes $\tau(z)$ and $F_z(z)$, and the length $L(z)$ instead of their surface values.

Using Eqs. (22) and (56), we can relate ς and $\tilde Z$ for stably stratified turbulence as

$$\varsigma = \frac{\tilde Z\, \tilde E_{\rm K}^{1/2}}{\kappa_0\, (1 + C_\Phi - \tilde Z\, \tilde E_{\rm K}^{1/2}/R_\infty)}. \tag{59}$$

For the surface layer ($\tilde Z \ll 1$) in stably stratified turbulence, the dimensionless height $\varsigma = z/L$. In this case the normalised TKE is $\tilde E_{\rm K} \approx 1$ [see Eq. (11)], so that Eq. (59) is reduced to

$$\frac{z}{L} = \frac{\tilde Z}{\kappa_0\, (1 + C_\Phi)}. \tag{60}$$

This equation coincides with Eq. (13) derived for the low part ($|\tilde Z| \ll 1$) of the surface layer in convective turbulence.

V. SURFACE LAYERS IN CONVECTIVE TURBULENCE

In this section we apply results obtained in Section III to convective turbulence. In this case, the nonlinear equation for the vertical profile of the normalized TKE, $\tilde E_{\rm K}(\tilde Z) = E_{\rm K}(\tilde Z)/E_{\rm K0}$ is given by Eq. (10). In Fig. 5 we show the normalized turbulent kinetic energy $E_{\rm K}^* = E_{\rm K}/u_*^2$ versus z/L obtained in the EFB theory. This dependence has been compared with the data [67] obtained

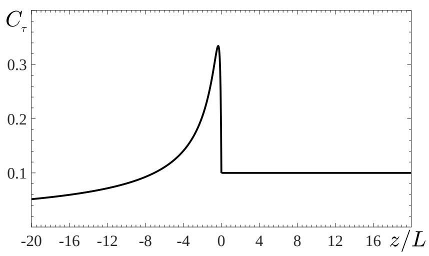

FIG. 6. The function C_τ versus z/L for convective and stably stratified turbulence.

from meteorological observations at the Eureka station located in the Canadian territory of Nunavut [68] in the conditions of long-lived convective boundary layer typical of the arctic summer. The better agreement between theoretical predictions and the observation data is achieved when C_τ is the following function of z/L (see Fig. 6):

$$C_\tau = \left(0.1 + \frac{1.72\,|X(z)|}{1+2|X(z)|}\right)\left(1+\frac{4z}{|L|}\right)^{-2/3}, \quad (61)$$

where $X(z) = \mathrm{Ri_f}(z)/\mathrm{R}_\infty$. We remind that C_τ is related to the effective dissipation time scale of the Reynolds stress.

Asymptotic solutions of Eq. (10) for the normalized TKE, $\tilde{E}_\mathrm{K}(\tilde{Z})$ are given by Eq. (11) for a lower part ($|\tilde{Z}| \ll 1$) of the surface convective layer, and by Eq. (12) for an upper part ($|\tilde{Z}| \gg 1$) of the surface convective layer. Below we present asymptotic formulas for various turbulent characteristics based on Eqs. (20), (22)–(26), (36)–(38), (41) and (51)–(52) for the lower and upper parts of the surface layer in convective turbulence. In particular, the turbulence characteristics for a lower part ($|\tilde{Z}| \ll 1$) of the surface convective layer are given by

- the flux Richardson number,

$$\mathrm{Ri_f} = -(1+C_\Phi)^{-1}\,|\tilde{Z}|, \quad (62)$$

- the large-scale shear,

$$S = \frac{u_*}{\kappa_0\, z}, \quad (63)$$

- the turbulent viscosity,

$$K_\mathrm{M} = \kappa_0\, u_*\, z, \quad (64)$$

- the vertical share of TKE,

$$A_z(\mathrm{Ri_f}) = A_z^{(0)} + \left(1 - A_z^{(0)}\right)|\tilde{Z}|, \quad (65)$$

- the turbulent Prandtl number,

$$\mathrm{Pr_T} = \mathrm{Pr_T^{(0)}}\left[1 - \frac{C_\theta\, C_\mathrm{p}}{A_z^{(0)}\,(1+C_\Phi)}\,|\tilde{Z}|\right], \quad (66)$$

- the level of temperature fluctuations,

$$\frac{E_\theta}{\theta_*^2} = C_\mathrm{p}\,\left(2C_\tau\, A_z^{(0)}\right)^{-1/2}\,\mathrm{Pr_T^{(0)}}\,\left(1 - C_\mathrm{E}\,|\tilde{Z}|\right), \quad (67)$$

- the vertical gradient of the mean potential temperature,

$$\nabla_z\overline{\Theta} = -\frac{\theta_*\,\mathrm{Pr_T^{(0)}}}{\kappa\, z}, \quad (68)$$

- the ratio of the horizontal and vertical turbulent fluxes of potential temperature,

$$\frac{F_i}{F_z} = -C_\mathrm{F}\,\left(2\,C_\tau\,A_z^{(0)}\right)^{-1/2}\left[1 - \frac{|\tilde{Z}|}{2A_z^{(0)}}\right], \quad (69)$$

- the horizontal components of TKE,

$$E_x = E_y = E_\mathrm{K0}\,\left(1 - A_z^{(0)}\right)\left(1 - \frac{1}{2}\,|\tilde{Z}|\right), \quad (70)$$

where

$$C_\mathrm{E} = \frac{1}{6}\left[1 + 2\left(A_z^{(0)}\right)^{-1}\right] + \frac{C_\theta\, C_\mathrm{p}}{A_z^{(0)}\,(1+C_\Phi)}. \quad (71)$$

In Eq. (63) we take into account that for the surface layer in convective turbulence, the vertical integral turbulent scale, $\ell_z = C_\ell\, z$ and in Eq. (69) we consider the case when the mean velocity $\overline{U}_i$ is directed along the x-axis.

For an upper part ($|\tilde{Z}| \gg 1$) of the surface convective layer, the turbulence characteristics are given by

- the flux Richardson number,

$$\mathrm{Ri_f} = -(1+C_\Phi)^{-1}\,\tilde{Z}^{4/3}, \quad (72)$$

- the large-scale shear,

$$S = \frac{u_*}{|L|}\,(1+C_\Phi)\,\tilde{Z}^{-4/3}, \quad (73)$$

- the turbulent viscosity,

$$K_\mathrm{M} = (1+C_\Phi)^{-1}\,u_*\,|L|\,\tilde{Z}^{4/3}, \quad (74)$$

- the normalized vertical integral scale ℓ_z,

$$\frac{\ell_z}{|L|} = (2C_\tau)^{-3/4}\,\tilde{Z}^{4/3}, \quad (75)$$

- the normalized TKE,

$$\frac{E_\mathrm{K}}{u_*^2} = (2C_\tau)^{-1/2}\,\tilde{Z}^{2/3}, \quad (76)$$

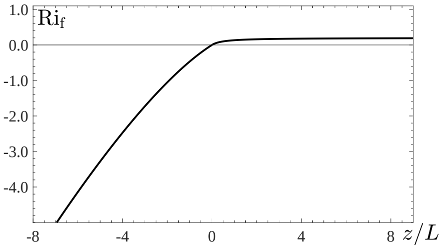

FIG. 7. The flux Richardson number $\mathrm{Ri_f}$ versus z/L for convective and stably stratified turbulence.

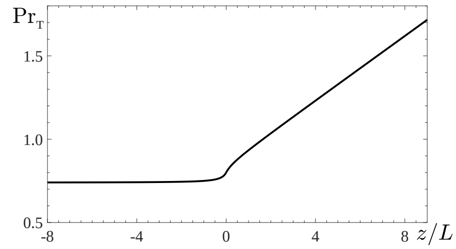

FIG. 8. The turbulent Prandtl number Pr_T versus z/L for convective and stably stratified turbulence.

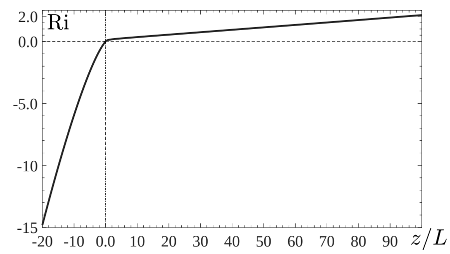

FIG. 9. The gradient Richardson number Ri versus z/L for convective and stably stratified turbulence.

- the vertical share of TKE,

$$A_z(\mathrm{Ri_f}) = 1 - \left(1 - A_z^{(0)}\right) \tilde{Z}^{-4/3}, \tag{77}$$

- the turbulent Prandtl number,

$$\mathrm{Pr_T} = \mathrm{Pr_T^{(\infty)}} \left[1 - \left(1 - \frac{\mathrm{Pr_T^{(\infty)}}}{\mathrm{Pr_T^{(0)}}}\right) \tilde{Z}^{-4/3}\right], \tag{78}$$

- the level of temperature fluctuations E_θ/θ_*^2,

$$\frac{E_\theta}{\theta_*^2} = C_\mathrm{p}\ (2C_\tau)^{-1/2}\, \mathrm{Pr_T^{(\infty)}}\, \tilde{Z}^{-2/3}, \tag{79}$$

- the vertical gradient of the mean potential temperature,

$$\nabla_z \overline{\Theta} = -\frac{\theta_*}{|L|}\, \mathrm{Pr_T^{(\infty)}}\, \tilde{Z}^{-4/3}, \tag{80}$$

- the ratio of the horizontal and vertical turbulent fluxes of potential temperature,

$$\frac{F_x}{F_z} = -C_\mathrm{F}\ (2\,C_\tau)^{-1/2}\ \tilde{Z}^{-2/3}, \tag{81}$$

- the horizontal components of TKE,

$$E_x = E_y = E_\mathrm{K0} \left(1 - A_z^{(0)}\right) \tilde{Z}^{-2/3}, \tag{82}$$

where

$$\mathrm{Pr_T^{(\infty)}} = \mathrm{Pr_T^{(0)}} \left[1 + \frac{C_\theta\, C_\mathrm{p}}{1 + C_\Phi}\right]^{-1}, \tag{83}$$

and in Eq. (81) we consider the case when the mean velocity $\overline{U}_i$ is directed along the x-axis.

Substituting Eq. (9) and the relation $\ell_z = C_\ell\, z$ into Eq. (76), we arrive at the famous expression for the convective turbulent energy,

$$E_\mathrm{K} = C_\mathrm{c}\, (\beta\, F_z\, z)^{2/3}, \tag{84}$$

obtained by Prandtl [69] using dimension analysis. Scalings for convective turbulence similar to Eqs. (72)–(74) and (79)–(80) (where $\ell_z = C_\ell\, z$), have been obtained by [69–71] using dimension analysis (see for a review books by [1, 2, 16]). The scalings similar to Eqs. (81)–(82) were derived using dimension analysis by [14, 15]. Most of the above scalings are in agreement with the data of the atmospheric observations discussed by [72].

In Figs. 7–16 we show vertical profiles of various turbulent characteristics for convective ($L < 0$) and stably stratified ($L > 0$) turbulence. These dependencies are based on Eqs. (8), (10), (13), (20), (22)–(26), (36)–(38), (41), (50)–(52) and (59). Three basic dimensional numbers, $\mathrm{Ri_f}$, Pr_T and Ri, plotted in Figs. 7–9, are related by the expression $\mathrm{Ri} = \mathrm{Ri_f}\, \mathrm{Pr}_T$.

Absolute values of the gradient Richardson number Ri in convective turbulence are much larger than in stably stratified turbulence. The reason is that the large-scale shear in convective turbulence is much smaller than in stably stratified turbulence (see Fig. 10). This is because TKE in convective turbulence is much stronger than in stably stratified turbulence (see Fig. 12), e.g, in convection, both, the buoyancy and large-scale shear produce turbulence. Contrary, in stably stratified turbulence, the large-scale shear produces TKE, while the buoyancy decreases TKE and produces the temperature fluctuations.

On the other hand, the normalized intensity of potential temperature fluctuations $\tilde{E}_\theta = E_\theta/\theta_*^2$ (see Fig. 13) in convective turbulence is much weaker than in stably stratified turbulence. The latter is caused by a weak gradient of the mean potential temperature in convective turbulence in comparison with that of stably stratified

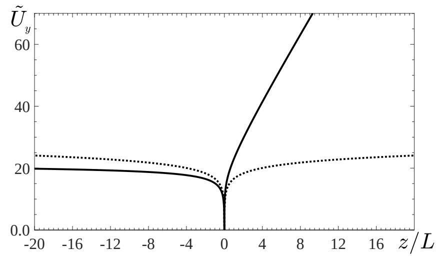

FIG. 10. The normalised mean velocity $\tilde{U}_y = \overline{U}_y/u_*$ (solid line) versus z/L for convective and stably stratified turbulence, where the normalised height of the roughness elements is $z_*/L = 5.28 \times 10^{-4}$. The dotted line corresponds to $\tilde{U}_y = \kappa^{-1} \ln(z/z_*)$.

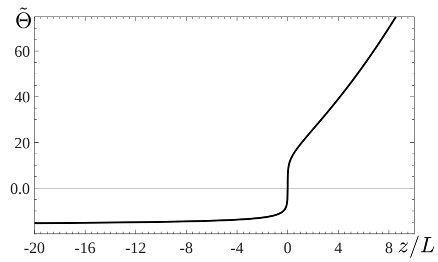

FIG. 11. The normalised mean temperature difference $\tilde{\Theta} = (\overline{T} - \overline{T}_b)/\theta_*$ versus z/L for convective and stably stratified turbulence, where $\overline{T}_b$ is the mean temperature at the lower boundary.

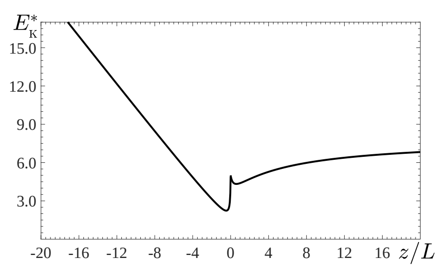

FIG. 12. The normalized turbulent kinetic energy $E_{\rm K}^* = E_{\rm K}/u_*^2$ versus z/L for convective and stably stratified turbulence.

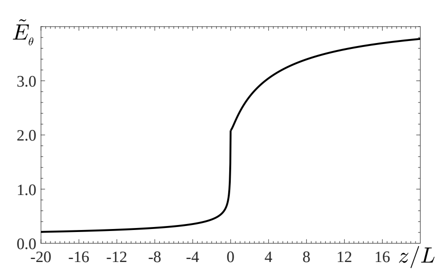

FIG. 13. The normalized intensity of potential temperature fluctuations $\tilde{E}_\theta = E_\theta/\theta_*^2$ versus z/L for convective and stably stratified turbulence.

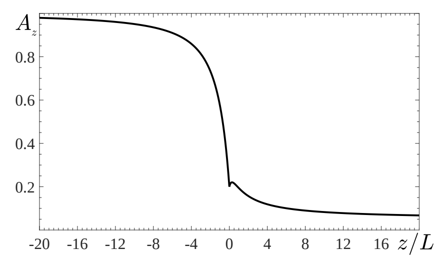

FIG. 14. The normalized vertical share A_z of turbulent kinetic energy versus z/L for convective and stably stratified turbulence.

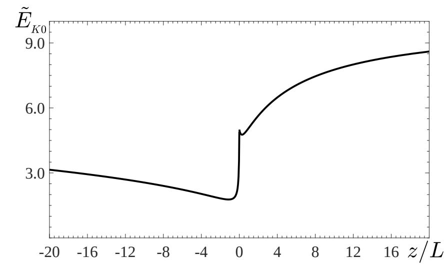

FIG. 15. The normalized turbulent kinetic energy $\tilde{E}_{\rm K0} = E_{\rm K0}/u_*^2$ versus z/L for convective and stably stratified turbulence.

turbulence (see Fig. 11). The vertical share A_z of turbulent kinetic energy in stably stratified turbulence is changed stronger than in the surface layers of convective turbulence (see Fig. 14). Indeed, turbulence tends to be two-dimension for very large gradient Richardson number in stably stratified turbulence, i.e., A_z becomes very small. Contrary, in convection the buoyancy is dominated in the energy production in the upper part of the surface layer, resulting in a strong increase of the vertical TKE, i.e., the vertical share $A_z \to 1$.

Since the normalized turbulent kinetic energy $\tilde{E}_{\rm K0} = E_{\rm K0}/u_*^2$ is inversely proportional to the vertical share A_z, it changes significantly in stably stratified turbulence in comparison with convective turbulence (see Fig. 15). In Fig. 16 we show the normalized vertical integral scale ℓ_z/L versus z/L for convective and stably stratified turbulence. In stably stratified turbulence, the vertical inte-

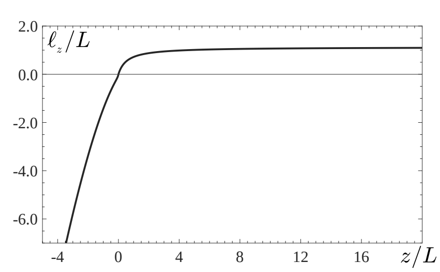

FIG. 16. The normalized vertical integral scale ℓ_z/L versus z/L for convective and stably stratified turbulence.

gral scale reaches the Obukhov length scale at high gradient Richarson numbers. Contrary, in convective turbulence the ratio $\ell_z/|L|$ is strongly increases with height.

VI. CONCLUSIONS

We develop a unified theory for the atmospheric surface layers in turbulent convection and stably stratified turbulence. This theory is based on the energy- and flux budget turbulence closure model that uses the budget equations for turbulent energies and fluxes. In the framework of this theory we determine the vertical profiles for all turbulent characteristics and for the mean velocity and mean potential temperature. In particular, we find the vertical profiles of turbulent kinetic energy, the intensity of turbulent potential temperature fluctuations, the vertical turbulent fluxes of momentum and buoyancy (proportional to potential temperature), the integral turbulence scale, the turbulent anisotropy, the turbulent Prandtl number and the flux Richardson number.

Since the large-scale shear in convective turbulence is much smaller than in stably stratified turbulence, the absolute values of the gradient Richardson number in convective turbulence are much larger than in stably stratified turbulence. This is natural result, since turbulent kinetic energy (produced by both, the buoyancy and large-scale shear) in convective turbulence is much stronger than in stably stratified turbulence. On the other hand, the large-scale shear produces turbulent kinetic energy in stably stratified turbulence, and the buoyancy decreases TKE and produces the temperature fluctuations. In convective turbulence, the gradient of the mean potential temperature is usually small in comparison with stably stratified turbulence. Therefore, potential temperature fluctuations are much smaller than in stably stratified turbulence. The vertical integral scale in stably stratified turbulence can only reach the Obukhov length scale at high gradient Richarson numbers. On the other hand, the vertical integral scale in convective turbulence can be much larger than the absolute value of the Obukhov length scale.

ACKNOWLEDGMENTS

This paper is dedicated to Prof. Sergej Zilitinkevich (1936-2021) who initiated this work and discussed the obtained results. This research was supported in part by the PAZY Foundation of the Israel Atomic Energy Commission (grant No. 122-2020), the Israel Ministry of Science and Technology (grant No. 3-16516) and the Academy of Finland (grant No. 314 798/799).

[1] A. S. Monin and A. M. Yaglom, *Statistical Fluid Mechanics*, Vol. 1 (MIT Press, 1971).
[2] A. S. Monin and A. M. Yaglom, *Statistical Fluid Mechanics*, Vol. 2 (Courier Corporation, 2013).
[3] W. D. McComb, *The Physics of Fluid Turbulence* (Oxford Science Publications, 1990).
[4] U. Frisch, *Turbulence: the Legacy of A. N. Kolmogorov* (Cambridge University Press, Cambridge, 1995).
[5] S. B. Pope, *Turbulent Flows* (Cambridge University Press, Cambridge, 2000).
[6] M. Lesieur, *Turbulence in Fluids* (Springer, 2008).
[7] P. A. Davidson, *Turbulence in Rotating, Stratified and Electrically Conducting Fluids* (Cambridge University Press, Cambridge, 2013).
[8] I. Rogachevskii, *Introduction to Turbulent Transport of Particles, Temperature and Magnetic Fields* (Cambridge University Press, Cambridge, 2021).
[9] A. N. Kolmogorov, Dissipation of energy in the locally isotropic turbulence, Dokl. Akad. Nauk SSSR A **32**, 16 (1941).
[10] A. N. Kolmogorov, Energy dissipation in locally isotropic turbulence, Dokl. Akad. Nauk. SSSR A **32**, 19 (1941).
[11] A. N. Kolmogorov, The equations of turbulent motion in an incompressible fluid, Izvestia Akad. Sci., USSR; Phys. **6**, 56 (1942).
[12] A. N. Kolmogorov, The local structure of turbulence in incompressible viscous fluid for very large reynolds numbers, Proc. Roy. Soc. London A **434**, 9 (1991).
[13] S. Zilitinkevich, E. Kadantsev, I. Repina, E. Mortikov, and A. Glazunov, Order out of chaos: Shifting paradigm of convective turbulence, J. Atmosph. Sci. **78**, 3925 (2021).
[14] S. S. Zilitinkevich, Turbulence and diffusion in free convection, Izv. Acad. Sci. USSR Atmos. Ocean. Phys. **7**, 825 (1971).
[15] S. S. Zilitinkevich, Shear convection, Boundary-Layer Meteor., **3**, 416 (1973).
[16] S. S. Zilitinkevich, *Turbulent Penetrative Convection* (Aldershot: Avebury Technical, 1991).
[17] S. Zilitinkevich, J. Hunt, I. N. Esau, A. Grachev, D. Lalas, E. Akylas, M. Tombrou, C. Fairall, H. Fernando, A. Baklanov, *et al.*, The influence of large convective eddies on the surface-layer turbulence, Quart. J. Roy. Meteorolog. Soc. **132**, 1426 (2006).
[18] J. Wyngaard and O. Coté, The budgets of turbulent kinetic energy and temperature variance in the atmospheric surface layer, J. Atmosph. Sci. **28**, 190 (1971).
[19] B. Kader and A. Yaglom, Mean fields and fluctuation moments in unstably stratified turbulent boundary layers, J. Fluid Mech. **212**, 637 (1990).
[20] T. Elperin, N. Kleeorin, I. Rogachevskii, and S. Zilitinkevich, Formation of large-scale semi-organized structures in turbulent convection, Phys. Rev. E **66**, 066305 (2002).
[21] T. Elperin, N. Kleeorin, I. Rogachevskii, and S. Zilitinkevich, Tangling turbulence and semi-organized structures in convective boundary layers, Boundary-Layer Meteorol. **119**, 449 (2006).
[22] T. Elperin, I. Golubev, N. Kleeorin, and I. Rogachevskii, Large-scale instabilities in a nonrotating turbulent convection, Phys. Fluids **18**, 126601 (2006).

[23] A. Glazunov and V. Dymnikov, Spatial spectra and characteristic horizontal scales of temperature and velocity fluctuations in the convective boundary layer of the atmosphere, Izv. Atmos. Ocean. Phys. **49**, 33 (2013).

[24] T. Banerjee, G. Katul, S. Salesky, and M. Chamecki, Revisiting the formulations for the longitudinal velocity variance in the unstable atmospheric surface layer, Quart. J. Roy. Meteorolog. Soc. **141**, 1699 (2015).

[25] S. T. Salesky, M. Chamecki, and E. Bou-Zeid, On the nature of the transition between roll and cellular organization in the convective boundary layer, Boundary-Layer Meteorol. **163**, 41 (2017).

[26] S. Salesky and W. Anderson, Buoyancy effects on large-scale motions in convective atmospheric boundary layers: implications for modulation of near-wall processes, J. Fluid Mech. **856**, 135 (2018).

[27] S. Salesky and W. Anderson, Coherent structures modulate atmospheric surface layer flux-gradient relationships, Phys. Rev. Lett. **125**, 124501 (2020).

[28] S. S. Zilitinkevich, T. Elperin, N. Kleeorin, and I. Rogachevskii, Energy- and flux budget (efb) turbulence closure model for stably stratified flows. part i: Steady-state, homogeneous regimes, Boundary-Layer Meteorol. **125**, 167 (2007).

[29] S. S. Zilitinkevich, T. Elperin, N. Kleeorin, I. Rogachevskii, I. Esau, T. Mauritsen, and M. W. Miles, Turbulence energetics in stably stratified geophysical flows: Strong and weak mixing regimes, Quarterly J. Roy. Meteorol. Soc. **134**, 793 (2008).

[30] S. S. Zilitinkevich, T. Elperin, N. Kleeorin, V. L'vov, and I. Rogachevskii, Energy-and flux-budget turbulence closure model for stably stratified flows. part ii: the role of internal gravity waves, Boundary-Layer Meteorol. **133**, 139 (2009).

[31] S. S. Zilitinkevich, I. Esau, N. Kleeorin, I. Rogachevskii, and R. D. Kouznetsov, On the velocity gradient in stably stratified sheared flows. part 1: asymptotic analysis and applications, Boundary-Layer Meteorol. **135**, 505 (2010).

[32] S. S. Zilitinkevich, T. Elperin, N. Kleeorin, I. Rogachevskii, and I. Esau, A hierarchy of energy- and flux-budget (efb) turbulence closure models for stably stratified geophysical flows, Boundary-Layer Meteorol. **146**, 341 (2013).

[33] N. Kleeorin, I. Rogachevskii, I. A. Soustova, Y. I. Troitskaya, O. S. Ermakova, and S. Zilitinkevich, Internal gravity waves in the energy and flux budget turbulence-closure theory for shear-free stably stratified flows, Phys. Rev. E **99**, 063106 (2019).

[34] N. Kleeorin, I. Rogachevskii, and S. Zilitinkevich, Energy and flux budget closure theory for passive scalar in stably stratified turbulence, Phys. Fluids **33**, 076601 (2021).

[35] T. Mauritsen, G. Svensson, S. S. Zilitinkevich, I. Esau, L. Enger, and B. Grisogono, A total turbulent energy closure model for neutrally and stably stratified atmospheric boundary layers, J. Atmos. Sci. **64**, 4113 (2007).

[36] B. Galperin, S. Sukoriansky, and P. S. Anderson, On the critical richardson number in stably stratified turbulence, Atmosph. Sci. Lett. **8**, 65 (2007).

[37] V. Canuto, Y. Cheng, A. Howard, and I. Esau, Stably stratified flows: A model with no ri (cr), Journal of the atmospheric sciences **65**, 2437 (2008).

[38] V. S. L'vov, I. Procaccia, and O. Rudenko, Turbulent fluxes in stably stratified boundary layers, Physica Scripta **2008**, 014010 (2008).

[39] S. Sukoriansky and B. Galperin, Anisotropic turbulence and internal waves in stably stratified flows (qnse theory), Physica Scripta **2008**, 014036 (2008).

[40] H. Savijärvi, Stable boundary layer: Parametrizations for local and larger scales, Quart. J. Roy. Meteorolog. Soc. **135**, 914 (2009).

[41] L. Kantha and S. Carniel, A note on modeling mixing in stably stratified flows, J. Atmosph. Sci. **66**, 2501 (2009).

[42] Y. Kitamura, Modifications to the mellor-yamada-nakanishi-niino (mynn) model for the stable stratification case, J. Meteorolog. Soc. Japan. Ser. II **88**, 857 (2010).

[43] D. Li, G. G. Katul, and S. S. Zilitinkevich, Closure schemes for stably stratified atmospheric flows without turbulence cutoff, J. Atmosph. Sci. **73**, 4817 (2016).

[44] D. Li, Turbulent prandtl number in the atmospheric boundary layer-where are we now?, Atmosph. Res. **216**, 86 (2019).

[45] J. C. Kaimal and J. J. Finnigan, *Atmospheric Boundary Layer Flows: Their Structure and Measurement* (Oxford University press, 1994).

[46] L. Ostrovsky and Y. I. Troitskaya, A model of turbulent transfer and dynamics of turbulence in a stratified shear-flow, Izv. Atmos. Ocean. Phys. **23**, 1031 (1987).

[47] V. Canuto and F. Minotti, Stratified turbulence in the atmosphere and oceans: A new subgrid model, J. Atmosph. Sci. **50**, 1925 (1993).

[48] V. S. L'vov, I. Procaccia, and O. Rudenko, Energy conservation and second-order statistics in stably stratified turbulent boundary layers, Environmental Fluid Mechanics **9**, 267 (2009).

[49] J. C. Rotta, Statistische theorie nichthomogener turbulenz, Zeitschrift für Physik **129**, 547 (1951).

[50] J. Kondo, O. Kanechika, and N. Yasuda, Heat and momentum transfers under strong stability in the atmospheric surface layer, J. Atmosph. Sci. **35**, 1012 (1978).

[51] F. Bertin, J. Barat, and R. Wilson, Energy dissipation rates, eddy diffusivity, and the prandtl number: An in situ experimental approach and its consequences on radar estimate of turbulent parameters, Radio Science **32**, 791 (1997).

[52] C. R. Rehmann and J. R. Koseff, Mean potential energy change in stratified grid turbulence, Dynamics of Atmospheres and Oceans **37**, 271 (2004).

[53] Y. Ohya, Wind-tunnel study of atmospheric stable boundary layers over a rough surface, Boundary-Layer Meteorol. **98**, 57 (2001).

[54] E. J. Strang and H. J. S. Fernando, Vertical mixing and transports through a stratified shear layer, J. Phys. Oceanogr. **31**, 2026 (2001).

[55] D. D. Stretch, J. W. Rottman, S. K. Venayagamoorthy, K. K. Nomura, and C. R. Rehmann, Mixing efficiency in decaying stably stratified turbulence, Dynamics of Atmospheres and Oceans **49**, 25 (2010).

[56] L. Mahrt and D. Vickers, Boundary-layer adjustment over small-scale changes of surface heat flux, Boundary-Layer Meteorology **116**, 313 (2005).

[57] T. Uttal, J. A. Curry, M. G. McPhee, D. K. Perovich, R. E. Moritz, J. A. Maslanik, P. S. Guest, H. L. Stern, J. A. Moore, R. Turenne, *et al.*, Surface heat budget of the arctic ocean, Bulletin of the American Meteorological Society **83**, 255 (2002).

[58] G. S. Poulos, W. Blumen, D. C. Fritts, J. K. Lundquist, J. Sun, S. P. Burns, C. Nappo, R. Banta, R. Newsom, J. Cuxart, *et al.*, Cases-99: A comprehensive investiga-

tion of the stable nocturnal boundary layer, Bulletin of the American Meteorological Society **83**, 555 (2002).
[59] R. Banta, R. Newsom, J. Lundquist, Y. Pichugina, R. Coulter, and L. Mahrt, Nocturnal low-level jet characteristics over kansas during cases-99, Boundary-Layer Meteorology **105**, 221 (2002).
[60] T. Elperin, N. Kleeorin, and I. Rogachevskii, Isotropic and anisotropic spectra of passive scalar fluctuations in turbulent fluid flow, Phys. Rev. E **53**, 3431 (1996).
[61] S. W. Churchill, A reinterpretation of the turbulent prandtl number, Industrial & Engineering Chemistry Research **41**, 6393 (2002).
[62] T. Foken, 50 years of the monin–obukhov similarity theory, Boundary-Layer Meteorology **119**, 431 (2006).
[63] L. H. Shih, J. R. Koseff, J. H. Ferziger, and C. R. Rehmann, Scaling and parameterization of stratified homogeneous turbulent shear flow, J. Fluid Mech. **412**, 1 (2000).
[64] D. Chung and G. Matheou, Direct numerical simulation of stationary homogeneous stratified sheared turbulence, J. Fluid Mech. **696**, 434 (2012).
[65] A. Monin and A. Obukhov, Basic laws of turbulent mixing in the atmosphere near the ground, Proc. Geophys. Inst. Academy of Science USSR (Tr. Geofiz. Inst., Akad. Nauk SSSR) **24**, 163 (1954).
[66] F. T. M. Nieuwstadt, The turbulent structure of the stable, nocturnal boundary layer, J. Atmosph. Sci. **41**, 2202 (1984).
[67] Kadantsev, E., and I. Repina, 2020: Meteorological observations of quasi-stationary long-lived convective boundary layers. EUDAT, accessed 20 August 2019, https://doi.org/10.23728/b2share.bb8964ff899c4711a0e8875b87ab2800.
[68] A. A. Grachev, P. O. G. Persson, T. Uttal, E. A. Akish, C. J. Cox, S. M. Morris, C. W. Fairall, R. S. Stone, G. Lesins, A. P. Makshtas, *et al.*, Seasonal and latitudinal variations of surface fluxes at two arctic terrestrial sites, Climate Dynamics **51**, 1793 (2018).
[69] L. Prandtl, Meteorologishe anwendungen der stromungslehre, Beitr. Phys. Atmos. **19**, 188 (1932).
[70] A. Obukhov, Turbulence in an atmosphere with a non-uniform temperature, Proc. Geophys. Inst. Academy of Science USSR (Tr. Geofiz. Inst., Akad. Nauk. SSSR) **1**, 95 (1946).
[71] A. Obukhov, Turbulence in an atmosphere with a non-uniform temperature, Boundary-Layer Meteorol. **2**, 7 (1971).
[72] B. Kader and A. Yaglom, Spectra and correlation functions of surface layer atmospheric turbulence in unstable thermal stratification, in *Turbulence and coherent structures* (Springer, 1991) pp. 387–412.